Available online at www.sciencedirect.com

ScienceDirect

Advances in Space Research 65 (2020) 2216–2222

ADVANCES IN SPACE RESEARCH (a COSPAR publication)

www.elsevier.com/locate/asr

Simulation of 500 MeV neutrons by using NaCl doped Water Cherenkov detector

Iván Sidelnik [a,b,e,*], Hernán Asorey [b,d,e], Nicolás Guarín [b], Mauricio Suaréz Durán [c], Mariano Gómez Berisso [a,b,e], José Lipovetzky [a,b,d,e], Juan Jerónimo Blostein [a,b,e]

[a] Consejo Nacional de Investigaciones Científicas y Técnicas (CONICET), Argentina
[b] Instituto Balseiro, CNEA-UNCuyo, Argentina
[c] Universidad Industrial de Santander, Bucaramanga, Colombia
[d] Comisión Nacional de Energía Atómica (CNEA) and Escuela de Tecnología y Medio Ambiente, UNRN, Argentina
[e] Centro Atómico Bariloche, Av.Bustillo 9500, S. C. Bariloche 8400, Argentina

Received 17 May 2019; received in revised form 18 February 2020; accepted 22 February 2020
Available online 3 March 2020

Abstract

In this work we show the capabilities of a water Cherenkov detector (WCD) to detect high energy neutrons. We present the simulation of the response of a doped WCD to 500 MeV monochromatic neutrons using Geant4. To do this, a detailed model of the WCD has been implemented. The active volume of the detector is composed of pure water and different concentrations of a ^{35}Cl based additive. The addition of this dopant shows an enhancement in the detection of high energetic neutrons. The sensitivity of this detector to neutrons achieved in our simulations is a relevant result for cosmic rays and space weather studies.

Keywords: Neutron detection; Water Cherenkov detector; Cherenkov effect; Space weather

1. Introduction

Water Cherenkov detectors (WCD) of large volumes using ultra pure water as active volume, are sensitive to charged relativistic particles and high energy photons. These detectors are used in a variety of implementations: from a diversity of astrophysical studies to the detection of Special Nuclear Material (SNM) for homeland security. WCD are usually chosen because they are cheap, robust and have a large solid angle. These detector have been widely used for cosmic ray detection since the late sixties, Watson (2011). The LAGO Suárez-Durán et al. (2016); Asorey et al. (2018); Sidelnik (2016), Auger Abraham et al. (2004) and HAWC Joshi et al. (2018) collaborations use nowadays WCDs to measure changes in the flux of cosmic rays and relate them with solar activity indicators studying, for instance, Forbush decreases Suárez-Durán et al. (2016). This could point out that a ground based space weather oriented experiment, using neutron monitors to study low energy cosmic ray flux variations, can use WCD as an alternative detector. There has also been a growing interest in the measurement of neutrons with additives into the water to increase the response of these detectors. The Super Kamiokande collaboration, for example, has been testing different approaches to the use of gadolinium (Gd) in their very large WCD (50,000 ton) Mori (2013), Watanabe et al. (2009).

There are studies that found that the major change in low energy cosmic rays are produced by neutrons as a part of secondary showers produced by cosmic ray particles

* Corresponding author at: Consejo Nacional de Investigaciones Científicas y Técnicas (CONICET), Argentina.
E-mail address: sidelnik@cnea.gov.ar (I. Sidelnik).

https://doi.org/10.1016/j.asr.2020.02.024
0273-1177/

Table 1
Cross section, abundance and energy of the elements used in the active volume of detection according to Firestone et al. (2007).

Element	Abundance [%]	Cross section [b]	Energy [keV]	k_0
^{1}H	99.99	0.3326±0.0007	2223.25	1.0000
^{16}O	99.76	0.000189±0.000008	870.68	3.35 E-5
^{23}Na	100	0.527±0.007	472.202	0.0630
^{35}Cl	75.78	43.84±0.17	1164.87	0.762
			517.0730	0.648
			6110.842	0.563
^{37}Cl	24.22	0.553±0.017	2166.90	0.00486

Asorey et al. (2018), Calderón-Ardila et al. (2019). CORSIKA simulations performed by the LAGO Collaboration shows that for cosmic rays that have its primary energy in the 10^{11} eV to 10^{15} eV range, and for different altitudes[1], the flux of secondaries is dominated by neutrons, with a spectrum that has a peak at 500 MeV Asorey et al. (2018), Calderón-Ardila et al. (2019), extending beyond the GeV. For this reason we choose the primary neutron energy of 500 MeV to run the present study.

Our choice is to use a ^{35}Cl based compound as an additive to the water, mainly because this isotope has a high cross Section (43.84±0.17 barns) for neutron absorption and a gamma prompt emission in cascade with a maximum of ~8578.6 keV Firestone et al. (2007). For this reason NaCl salt was selected to be used in the water Cherenkov detector, not only for the mentioned advantages of the Cl, but it is also a compound that can be easily dissolved in water, is cheap, and it is not contaminant if spilled, unlike Gd. WCD results ideal to detect high energy neutrons because of the neutron moderation capability of water.

In Table 1 the main elements used in the active volume of the detector are showed, as long as the corresponding abundance and neutron absorption cross sections with the most energetic prompt gamma line. The intensity of the prompt gamma lines emitted are determined by the neutron absorption probability as well as the line yield. In order to take into account both values simultaneously, a k_0 value is computed as the product of the line yield and the neutron absorption cross section. The k_0 value for a gamma ray emitted from each isotope is defined relative to that of ^{1}H, see details in Firestone et al. (2007). In order to take into account both magnitudes a k_0 is commonly used. Table 1 shows the most intense value of k_0 for each isotope,

It can be seen in Table 1 that the most intense lines are the 2223 keV from ^{1}H and the three lines from ^{35}Cl. It must be noted that the k_0 value reported are nuclear parameters. In each simulated configuration the Geant4 code takes into account not only these values, but also the number of nuclei per unit volume.

[1] Calderón-Ardila et al. (2019) show simulations for a site at La Serena, Chile 28 m a.s.l and at Chacaltaya, Bolivia, 5240 m a.s.l.

Our group has been working in neutron detection with WCD that uses pure water Sidelnik et al. (2017) and with NaCl as additive Sidelnik et al. (2019) using neutron sources that reaches energies of ~15 MeV. In this work we present the study of a WCD of 1 m^3 for neutron detection comparing the use of pure water and a non contaminant additive (NaCl) with a single PMT for 500 MeV impinging neutrons.

In Section 2 we describe the characteristics of the simulation performed with Geant4. Section 3 shows the results obtained, and finally, the conclusions are presented in Section 4.

2. Geant4 simulation scheme

We performed a detailed simulation of all the particle production physics and the detector geometry using Geant4 Allison et al. (2016). The detector is composed of a 96-cm-diameter by 133-cm-tall cylinder made of a of 0.5-m-thick stainless steel sheet. Depending on the selected configuration, the cylinder is filled with pure water or water with different concentrations of NaCl. Located inside at the top and center of the detector, there is a spherical section of h = 5 cm and 10.16 cm radii that simulates the surface detection of the photomultiplier tube (PMT). Between the water and the stainless steel volume there is a thin layer (with approximately 0.12 mm of thickness) that has the reflective and refractive properties of Tyvek® that enhances the propagation of Cherenkov photons inside the detector Filevich et al. (1999). A scheme of the simulated detector can be seen in Fig. 1, with a possible reaction of a neutron being moderated and absorbed inside the active volume. For the simulation it was used the Quantum Efficiency (QE) reported by Hamamatsu for the R5912 8" PMT Hamamatsu (2018), to sort the acceptance or rejection of a Cherenkov photon in the PMT, that contribute to the signal. The QE of a PMT is the probability that one Cherenkov photon is converted in one photoelectron into the cathode of the PMT. For the considered PMT it is around 25–30%. This probability is sorted in the simulation, accepting or rejecting Cherenkov photons as a contribution of the signal.

The simulations were performed considering 500 MeV monochromatic neutrons impinging horizontally at the middle of the height of the detector and 1 cm far away from

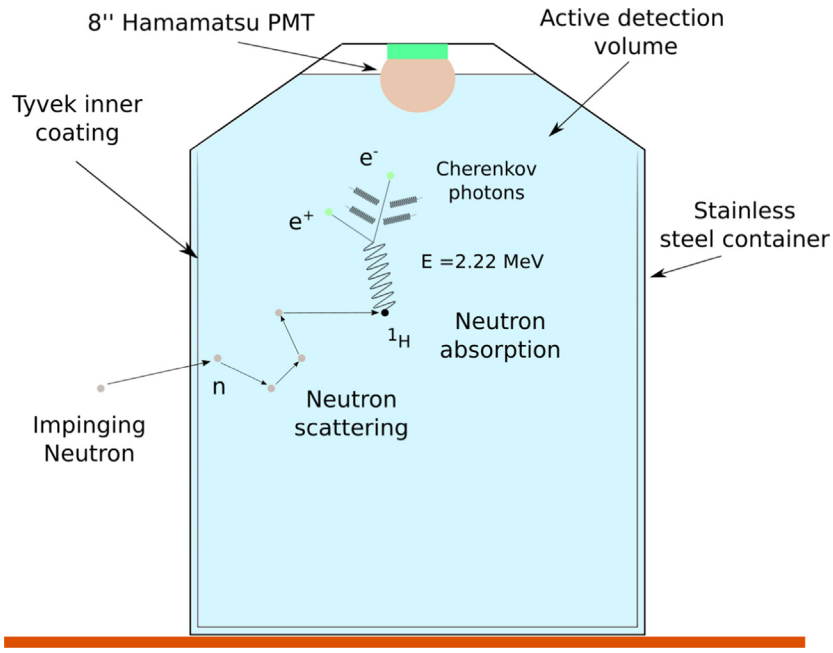

Fig. 1. Schematic view of the water Cherenkov detector setup with an impinging 500 MeV neutron. When a neutron enters into the WCD active volume (in light blue) it is moderated by the H_2O, and absorbed mainly by the dopant or hydrogen nucleous. The prompt gammas emitted after the neutron absorption produce electrons mainly by Compton scattering and pair production effects. In some cases these electrons have energies above the Cherenkov threshold thus producing photons that can reach the PMT.

the exterior border. As an active volume pure water (H_2O) and water with different NaCl concentrations, 2.5%, 5% and 10%, in mass was used.

3. Results and discussion

Simulations in Geant4 were performed including all the relevant parameters of the detector (listed in Section 2) injecting 150000 neutrons. First we aimed to understand the absorption process of the neutrons, comparing H_2O and including NaCl in different concentrations. In Table 2 we show the fraction of neutron captures within the active volume for the case of pure water and water with NaCl additive and the maximum absorption distance.

After a moderation process of the neutron in the water, it looses almost all its energy in a short distance, the particle is captured most of the times, either by the H^1 or the Cl^{35}, when is present. As the content of Cl increases, the neutron absorption result closest to the border of the detector. Beacuse there are more isotopes with larger cross section than H, the neutrons are absorved very close to the entry point of the detector.

Table 2
Total captures of neutrons and distance of maximum absorptions from simulations, using 500 MeV monochromatic neutrons.

Sensitive volume	Neutron capture probability [%]	Max. absorption distance [cm]
H_2O	25.18	8.4±0.1
H_2O + 2.5% NaCl	26.73	8.0±0.1
H_2O + 5% NaCl	27.65	7.7±0.1
H_2O + 10% NaCl	29.26	7.3±0.1

Fig. 2 shows the distance from the edge of the detector for the impinging monochromatic 500 MeV neutron beam and the absorption point. The maximum for absorption is at (8.4±0.1) cm for the pure water case (red circles) and (8.0±0.1) cm, (7.7±0.1) cm, (7.3±0.1) cm, in case of adding NaCl (green squares for 2.5%, violet triangles up for 5% and yellow triangles down for 10% in mass, respectively). It is clear that the number of absorptions increases with the addition of NaCl, improving the detection efficiency without significantly affecting the moderation process in water.

Fig. 3 shows the photons emitted into the active volume of the detector from pure water and different NaCl concentrations after the interaction of 500 MeV neutrons. In this Figure it can be seen (as deltas) the most intense prompt gamma lines indicated in Table 1. Since in Fig. 3 it can be difficult to distinguish the different contributions, in Fig. 4 we show the same results, as a function of energy in cumulative energy bins from right to left. In the 10 MeV to 100 MeV gamma energy range it can be seen that the gamma produced are essentially the same regardless the additive. However, below 10 MeV (see Fig. 4 bottom) the gamma production increases with increasing NaCl concentration.

Fig. 5 shows the electrons produced inside the detector by the gammas after the interaction of 500 MeV neutrons within the detector. The Compton edge can be appreciated for the electrons produced in pure water by the 2223 keV gamma line (red line) at $E_{elec} \simeq 1994$ keV. In the case of

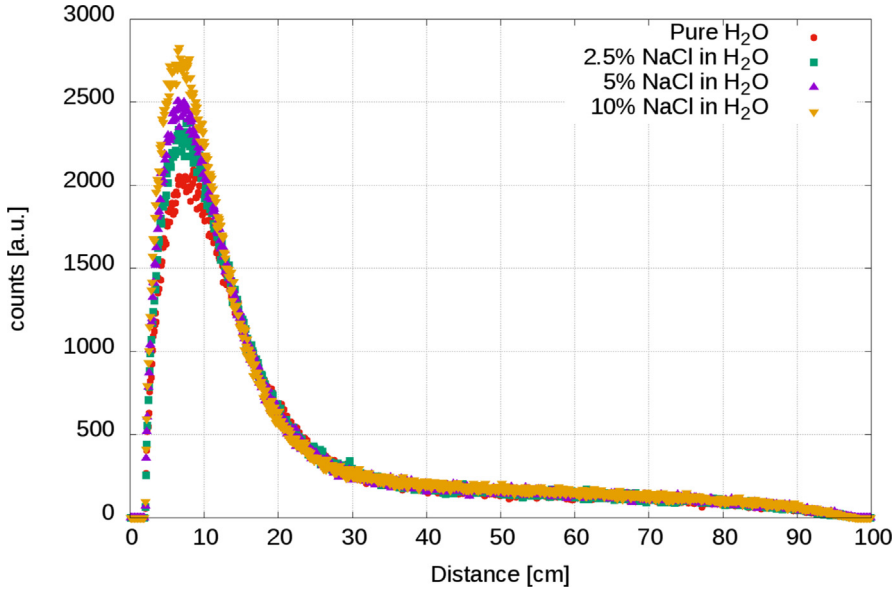

Fig. 2. Neutron captures of 500 MeV monochromatic neutron beam. The distance with the maximum number os neutron captures from the border of the detector (~8.4 cm) for water (red circles) and (~8.0 cm) for water with 2.5% of NaCl in mass concentration; ~7.7 cm for 5% and ~7.3 cm for 10%. The number of captures results larger due to the higher σ_{abs} of the ^{35}Cl. For further information see the text. (For interpretation of the references to colour in this figure legend, the reader is referred to the web version of this article.)

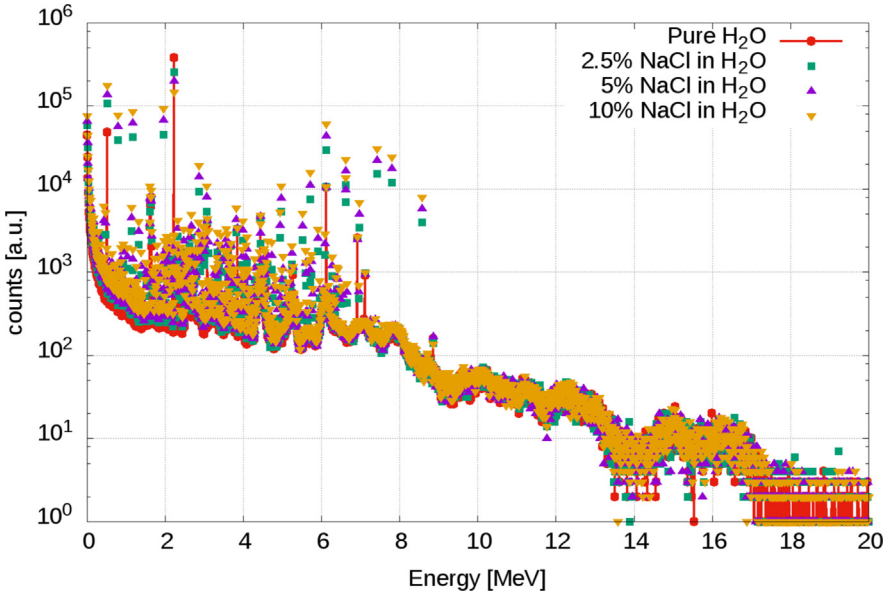

Fig. 3. Photon spectra emitted from pure water and different NaCl concentrations after the interaction of 500 MeV neutrons: pure water situation (red circles) and the different concentrations of NaCl, 2.5% (green squares), 5% (purple triangles up) and 10% (yellow triangles down). (For interpretation of the references to colour in this figure legend, the reader is referred to the web version of this article.)

water with different additive concentrations (green dashed, violet dashed-dot, and yellow dotted line) it can be seen that even if there are particles at higher energies, there is a Compton edge at $E_{elec} \simeq 8330$ keV, the maximum energy that an electron can have with a 8578.6 keV gamma particle (the maximum of the gamma emission) after a ^{35}Cl absorbs a neutron, and from that the mix of Compton edges at energy higher than 2223 keV that shows the increase of energetic electrons within the active volume of the detector. This means that even if the gammas are produced at very high energy, the most important contribution if the one that produces the electrons under ~10 MeV.

Fig. 6 shows the number of Cherenkov photons produced by the electrons showed in Fig. 5 that (considering the reflection on the Tyvek coating, and the water transparency) reach the PMT, and taking into account the QE

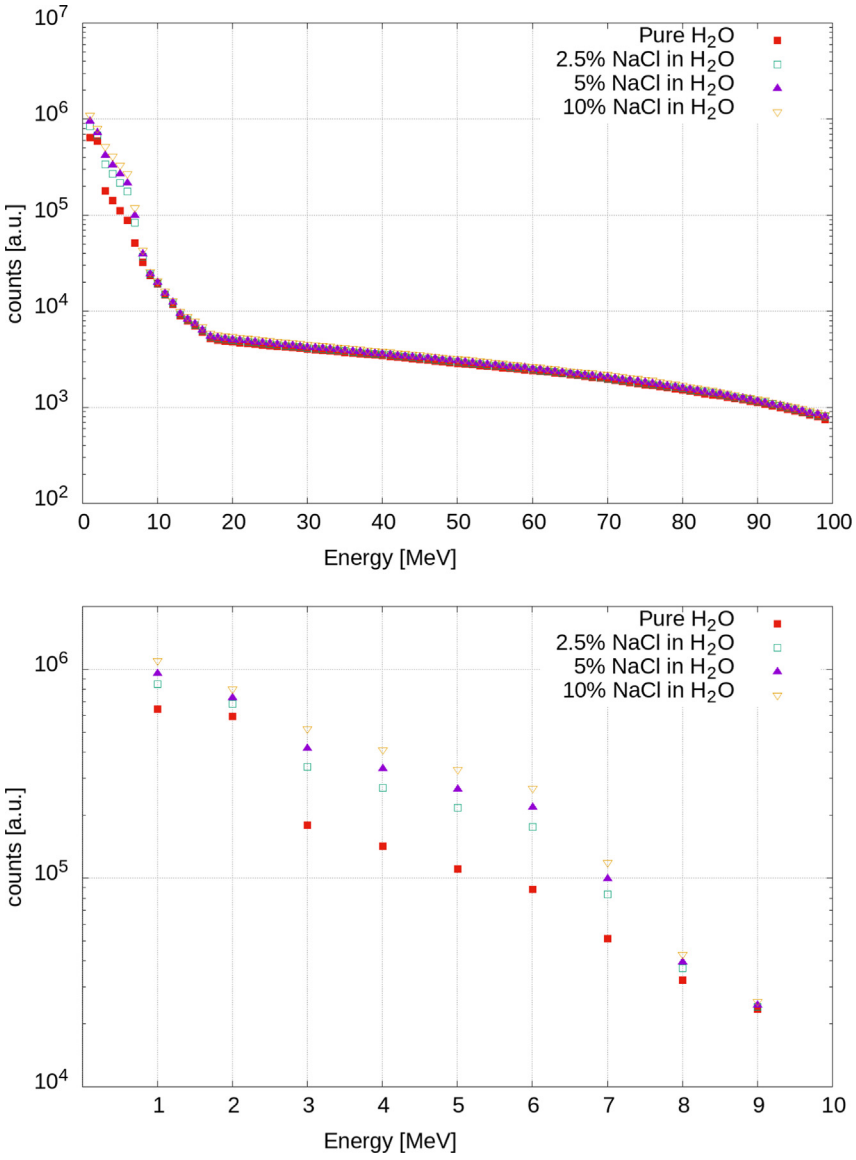

Fig. 4. Top: Gamma particles produced in the simulation after the interaction of 500 MeV monochromatic neutrons with pure water situation (red squares) and the different concentrations of NaCl, 2.5% (green empty squares), 5% (purple triangles up) and 10% (yellow triangles down) in cumulative energy bins from right to left. Bottom: zoom of the previous graphic below 10 MeV. (For interpretation of the references to colour in this figure legend, the reader is referred to the web version of this article.)

of the PMT photocathode produce a photoelectron that contributes to the signal. A more detailed review of the number of Cherenkov photons produced by electrons can be foun in reference Jackson (1999). For pure water (red continuous line) it can be seen that there are more events at low number of photons produced, this trend changes at ~100 number of photons. From 100 to 600 photons the doped water with different concentrations of NaCl (2.5% in green dashed lines, 5% in violet dash dot, and 10% in dotted yellow) produce more Cherenkov photons increasing the signal into the detector. Beyond 600 of photons produced, for impinging neutron energies there is no change regardless the concentration of NaCl into the active volume.

4. Conclusions

This work introduces results from simulations that shows in detail the physics of a WCD when high energetic neutrons enter into the detector active volume. We conclude that using a WCD with pure water as active volume, and a single PMT, 500 MeV neutrons can be detected. In addition, we have also shown that adding NaCl as dopant to the water the signal intensity increase, thus enhancing the capability for measure high energy neutrons. Being NaCl, cheap, non-toxic and easily accessible material, the results obtained are of interest for the development of neutron detectors for different applications. Of special importance are those related with space weather phenomena.

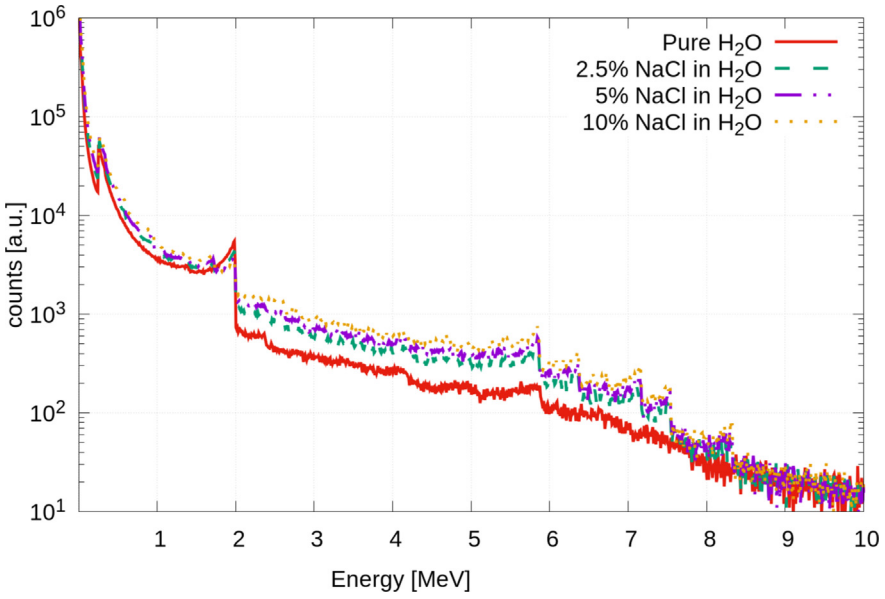

Fig. 5. Electrons spectrum produced inside the detector by the interaction of gammas within the active volume (Fig. 4), simulations performed using 500 MeV monochromatic neutrons.

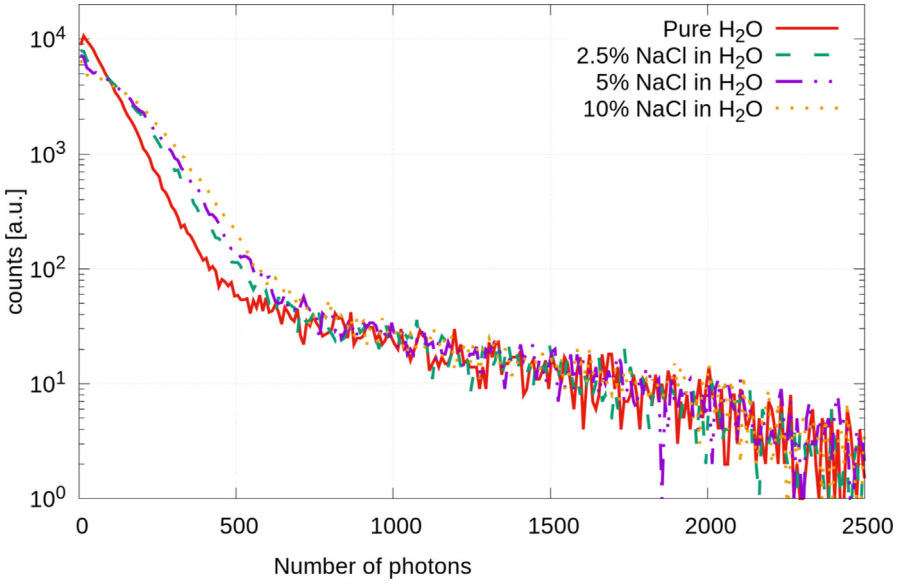

Fig. 6. Number of Cherenkov photons recorded in total accepted by the quantum efficiency of the PMT from those emitted by the electrons within the active volume of the detector.

Altought a more extensive analyses must be done widening the energy range, we conclude that WCD used as a neutron detector can be a complementary tool for standard neutron monitors based on He^3. These conclusions are relevant because WCD are widely used in the cosmic ray detection field. This arrangement presents a clear advantage over systems that employ Gd or other elements as dopant to increase the neutron signal, and more that one PMT, which have effects on the detector cost, operation simplicity, and contamination if its spilled.

Acknowledgment

The authors would like to acknowledge the full support by CONICET and CNEA. We are very thankful to the technicians in our lab that help to set up the detectors: P. D'avanzo, A. Mansilla, F. Y. Moreira, G. Anibal. This work has been done thanks to the following grants: PICT ANPCyT 2015-1644, PICT ANPCyT 2016-2096, PIP CONICET 2011 0552, UNCuyo Proy. Cod. 06/C483 and 06/C594.

References

Abraham, J., Aglietta, M., Aguirre, I.C., et al.Pierre Auger, 2004. Properties and performance of the prototype instrument for the Pierre Auger Observatory. Nucl. Instrum. Methods Phys. Res., Sect. A A523, 50–95. https://doi.org/10.1016/j.nima.2003.12.012.

Allison, J., Amako, K., Apostolakis, J., et al., 2016. Recent developments in Geant4. Nucl. Instrum. Methods Phys. Res., Sect. A 835, 186–225. https://doi.org/10.1016/j.nima.2016.06.125, URL http://www.sciencedirect.com/science/article/pii/S0168900216306957.

Asorey, H., Núñez, L.A., Suárez-Durán, M., 2018. Preliminary results from the latin american giant observatory space weather simulation chain. Space Weather 16, 461–475. https://doi.org/10.1002/2017SW001774.

Calderón-Ardila, R., Jaimes-Motta, A., Peña-Rodríguez, J., Sarmiento-Cano, C., Suárez-Durán, M., Vásquez-Ramírez, A.for the LAGO Collaboration (LAGO), 2019. Modeling the LAGO's detectors response to secondary particles at ground level from the Antarctic to Mexico. PoS ICRC2019, 412, URL https://pos.sissa.it/358/412/pdf.

Filevich, A., Bauleo, P., Bianchi, H., Martino, J.R., Torlasco, G., 1999. Spectral-directional reflectivity of Tyvek immersed in water. Nucl. Instrum. Methods Phys. Res., Sect. A 423, 108–118. https://doi.org/10.1016/S0168-9002(98)01194-2.

Firestone, R.B., Choi, H.D., Lindstrom, R.M., et al, 2007. Database of Prompt Gamma Rays from Slow Neutron Capture for Elemental Analysis. Number LBNL-55199 in Non-serial Publications, International Atomic Energy Agency, Vienna.

Hamamatsu, 2018. Permanent link to Hamamatsu Large Photocathode area datasheet. 323 pages, third edition. Technical Report TOTH9001E03a. https://www.hamamatsu.com/resources/pdf/etd/PMT_handbook_v3aE.pdf.

Jackson, J.D., 1999. Classical electrodynamics. 3rd, 808 pages, ed., John Wiley & Sons, New York, NY.

Joshi, V., Jardin-Blicq, A.for the HAWC Collaboration (HAWC), 2018. HAWC high energy upgrade with a sparse outrigger array. PoS ICRC2017, 806. https://doi.org/10.22323/1.301.0806, arXiv:1708.04032.

Mori, T.for the Super-Kamiokande Collaboration, 2013. Status of the Super-Kamiokande gadolinium project. Nucl. Instrum. Methods Phys. Res., Sect. A 732, 316–319. https://doi.org/10.1016/j.nima.2013.06.074.

Sidelnik, I.(LAGO), 2016. The Sites of the Latin American Giant Observatory. PoS ICRC2015, 665. https://doi.org/10.22323/1.236.0665.

Sidelnik, I., Asorey, H., Blostein, J.J., Berisso, M.G., 2017. Neutron detection using a water cherenkov detector with pure water and a single PMT. Nucl. Instrum. Methods Phys. Res. Section A: Accelerat., Spectromet., Detect. Associat. Equip. 876, 153–155. http://www.sciencedirect.com/science/article/pii/S0168900217302322, https://doi.org/10.1016/j.nima.2017.02.048. the 9th international workshop on Ring Imaging Cherenkov Detectors (RICH 2016), Bled, Slovenia, Sept. 5-9, 2016.

Sidelnik, I., Asorey, H., Guarin, N., Durán, M.S., Bessia, F.A., Arnaldi, L.H., Berisso, M.G., Lipovetzky, J., Pérez, M., Haro, M.S., Blostein, J.J., 2019. Neutron detection capabilities of water cherenkov detectors. Nucl. Instrum. Methods Phys. Res., Sect. A 952, 161962. https://doi.org/10.1016/j.nima.2019.03.017, URL http://www.sciencedirect.com/science/article/pii/S0168900219303158.

Suárez-Durán, M., Asorey, H., Dasso, S., Nunez, L., Peréz, Y., Sarmiento, C.(LAGO), 2016. The LAGO space weather program: directional geomagnetic effects, background fluence calculations and multi-spectral data analysis. PoS ICRC2015, 34–41. https://doi.org/10.22323/1.236.0142.

Watanabe, H., Zhang, H., Abe, K., et al., 2009. First study of neutron tagging with a water cherenkov detector. Astropart. Phys. 31, 320–328. https://doi.org/10.1016/j.astropartphys.2009.03.002, URL http://www.sciencedirect.com/science/article/pii/S0927650509000401.

Watson, A.A., 2011. The discovery of cherenkov radiation and its use in the detection of extensive air showers. Nucl. Phys. B Proc.Suppl. 212–213, 13–19. https://doi.org/10.1016/j.nuclphysbps.2011.03.003, proceedings of the Cosmic Ray International Seminars (CRIS 2010) 13-17 September 2010 Palazzo dei Chierici, Catania (Italy).